Construction and Building Materials 302 (2021) 124225

Contents lists available at ScienceDirect

Construction and Building Materials

journal homepage: www.elsevier.com/locate/conbuildmat

Binary blended cement pastes and concrete using gravel wash mud (GWM) powders

Vishojit Thapa, Danièle Waldmann *

Faculty of Science, Technology and Medicine (FSTM), University of Luxembourg, 6 avenue de la Fonte, L-4364 Esch-sur-Alzette, Luxembourg

ARTICLE INFO

Keywords:
Gravel wash mud
Concrete
SCM
Mechanical properties
Hydration kinetics
Carbonation

ABSTRACT

An alternative supplementary cementitious material (SCM) based on quarry waste sludge, namely gravel wash mud (GWM) powder, is investigated for its performance in blended cement pastes and concretes. Varying mix designs of blended cement pastes and concrete mixtures at Ordinary Portland cement (OPC) substitution degrees from 10 wt% up to 30 wt% by uncalcined and calcined GWM powders were examined at different curing ages using isothermal calorimetry, strength-based examinations, shrinkage test, carbonation test and scanning electron microscopy. The pozzolanic nature of the calcined GWM powder was confirmed, however, minor to no significant physiochemical contributions to the early hydration reactions were observed. The incorporation of calcined GWM powders up to OPC replacement levels of 20 wt% showed an enhancement of the long-term properties of the hardened specimens, namely less drying shrinkage and reduced progression of carbonation compared to the control mixtures. Beneficial strength-enhancing effects were observed for binary blended concrete mixes using calcined GWM powders at OPC replacement levels of 10 wt% and 20 wt% and classified them as viable proportions for alternative SCM-based concretes. The revalorisation of the GWM, a quarry waste product, as a novel and competitive raw material resource for cement production, would provide an environmental-friendly and alternative solution to the expensive and inefficient end-of-life scenario of GWM at the landfills.

1. Introduction

Concrete is incontestably the most used construction material, and it plays an essential role in the urbanisation of cities of industrialised countries as well as the rise of emerging countries to meet the living standards and the infrastructure requirements of rapidly growing populations worldwide, and its importance will continue to intensify in future [1]. The sustainable development of the construction industry has undoubtedly emerged to the focus of interest over the last decades as the progressive environmental consequences of the current concrete usage practices have further stimulated the urge for an appropriate and durable solution worldwide. Nonetheless, as the production of concrete is directly dependant on the acquirability of abundant local resources and their nature, current research outcomes are mainly able to come up with local up to regional solutions. The major portion of concrete's negative environmental impact is attributed to its principal binding agent, Ordinary Portland cement (OPC), whose production process, namely the clinkerisation process, generates high CO_2 emissions [2,3]. Current estimates state that the average yearly global cement production remained stable at around 4.1 Gt since 2013 [4–6]. However, the forecasts on the rise of the global population and its subsequent infrastructure development requirements suggest that global cement production will increase by more than 12% by 2050 [1].

Furthermore, the current expectations on the investigations and the advancements of the scientific and technological organisations collaborating with the cement industry are very high. The extent of the existing and future endeavours to mitigate the environmental impacts regarding the CO_2 emissions of the cement industry is correlated to the growing cement production rates and the speed of the technological progress of the sector. Therefore, various CO_2 mitigation strategies have been developed and established to formulate "eco-efficient" concretes [7]. One of the proposed solutions is the clinker replacement by "low carbon" constituents with proven binding properties, namely supplementary cementitious materials (SCMs), to reduce the environmental impacts and to improve the durability of concrete products without compromising its competitiveness [8,9]. Consequently, the current European cement standard EN 197–1 [10] authorises the incorporation of six supplementary main constituents (blast furnace slag, silica fume,

* Corresponding author.
E-mail address: daniele.waldmann@uni.lu (D. Waldmann).

https://doi.org/10.1016/j.conbuildmat.2021.124225
Received 3 November 2020; Received in revised form 2 July 2021; Accepted 10 July 2021
Available online 16 July 2021

pozzolana, fly ash, burnt shale and limestone) in addition to Portland cement clinker in the composition of common cement types. Moreover, for instance, the French national addition of the European concrete standard NF EN 206/CN [11] permits the use of Metakaolin as a pozzolanic addition for concrete after conformity according to the national product standard NF P18-513 [12]. There exist numerous research work on the physicochemical and mineralogical characteristics of these SCMs, the extent and intensity of the involved reaction mechanisms in the cement-based compounds, and their influence on the mechanical performance and durability of the resulting blended cements and concrete products [13–29].

However, in most of the European countries, not all of these constituents are abundantly available locally and the stocks of these traditional "mainstream" SCMs, mostly artificial pozzolans like silica fume (SF), fly ash (FA) or granulated blast furnace slag (GBS), are gradually disappearing as a result of more substantial sectoral and environmental restrictions, and technological advances in primary industrial sectors like the steel industry or the coal-fired power stations. This increasing scarcity of traditional SCMs and the already existing depletion of naturally mined materials has promoted the construction industry to research on new alternative SCMs worldwide, mostly originating from various industrial waste flows [24,30–33].

In recent years, there is a substantially growing research interest in the valorisation of co-products or wastes from quarries (washing sludge), abandoned clay mines (medium-reactive clay deposits) or other unused potential resources of diverse industrial origins to assess their aptitude for their use as SCMs in future blended cements and to provide larger flexibility to the local cement industry to encounter future challenges. Furthermore, the incorporation of these alternative waste-based SCMs in cementitious binders can reduce the environmental footprint of the quarries, and a potential stabilisation or even decrease of building materials' cost can be expected. A broad spectrum of local and regional industrial waste materials, which were not exploited to date and mainly landfilled, have been investigated to be incorporated as SCMs in blended cements or as additions in concrete. Among highly investigated waste products to reduce the clinker factor in future cements or to utilise as filler aggregates figure reservoir sludges [34], waste expanded perlites [35], waste glass sludges [36], granite quarry wastes [37], quarry wastes containing limestone, diabase and gneiss [38], quarry reservoir sludges [39–41], dolomitic quarry dust [42], marble stone dust [43], non-recyclable waste glass [44], ceramic wastes [44,45], clay-based construction wastes [46–48], and many more [49,50]. Most of the authors, researching the revalorisation of unutilised waste materials, report that independently of the reactivity of the waste-based SCMs, at lower replacement levels around 10 wt%, improved hydration kinetics and strength development of the blends are foreseeable. Furthermore, depending on the nature of reactivity (potential to possess respectively build hydraulic or pozzolanic binding properties, or both) and the intrinsic characteristics of the waste products, at OPC replacement levels around 20 wt%, the formation of additional hydration products at varying stages of the hydration process was observed, mostly leading to improved mechanical performances, reduced porosity (filling of micropores and improved interfacial transition zones), the enhancement of the microstructure and better durability (improved long-term behaviours and resistance to external deleterious effects) of the hardened products compared to the OPC-based reference mixtures [34–38,42–44,46–49]. Nonetheless, most of the studies consist of early investigations on the suitability of the waste material to be considered as SCM in binder mixtures or blended cement mortars.

2. Materials and experimental program

The objective of the conceptualised mix design and the applied experimental methods is to corroborate the performance of the proposed SCMs, namely GWM powders, to be incorporated in concrete mixtures as a promising alternative to only OPC-based concretes without compromising on the concrete's property requirements.

2.1. Materials and material preparations

A commercial Ordinary Portland cement (OPC; $\rho_{OPC} = 3.10$ kg/dm^3) with grade CEM I 42.5 R according to EN 197–1 [10] from Cimalux S.A. was used as the main binder of the different mixtures. The concrete mixtures were prepared with commercially available mixed sand and gravel aggregates of regional origin (Mosel sand and gravel mix, MSG; $\rho_{MSG} = 2.40$ kg/dm^3) with a grain size range of 0/16 mm, certified according to DIN EN 12620 [51]. The gravel wash mud was obtained from a Luxembourgish sandstone quarry (Carrières Feidt S.A.) and was pre-processed by desiccation to constant mass at 105 °C. After drying, the GWM chunks were powdered using a laboratory jaw breaker (no further powder milling process was required), hereafter referred to as the uncalcined GWM (UGWM; $\rho_{UGWM} = 2.52$ kg/dm^3) powder. The reproducibility and the consistency of the granulometry is confirmed. After the fine powders (UGWM) were set up for calcination. The calcined GWM (CGWM; $\rho_{UGWM} = 2.50$ kg/dm^3) powder was produced by thermal treatment of UGWM powder at 850 °C inside a laboratory chamber furnace (heating rate of about 5 °C/min) while maintaining the peak temperature for one hour, followed by a natural cooling down to room temperature. No further milling was done after the calcination process. The calcination allowed to transform the base material (UGWM) with low pozzolanic activity into a more amorphous and medium-reactive artificial pozzolan (CGWM) [39–41].

2.2. Mix design and curing conditions

2.2.1. Binder paste compositions

The mix proportions of the investigated binder pastes are presented in Table 1. Seven different cement paste mixes were prepared to incorporate increasing proportions of UGWM powders, respectively CGWM powders, from 10 wt% up to 30 wt%, and a reference mixture (REF). The water/binder (w/b) ratio was fixed to 0.4, and no additional aggregates were added. Three replicate specimens were prepared for each mixture, and the investigated curing ages were 28 and 56 days. The same mixing procedure was applied for all mixtures and carried out, as described in [40]. The mixtures were poured in steel moulds (40 × 40 × 160 mm^3) according to EN 196–1 [52]. After 24 h of hardening time, the specimens were demoulded, wrapped in cellophane foil to restrict moisture exchange with the surroundings and cured at ambient temperature until 24 h before the compression tests. For REF, UG20 and CG20, additional specimens were prepared to examine the evolution of compressive strengths from 1 day up to 90 days. Furthermore, the impact of curing conditions (cured in air and water) on the evolution of compressive strength of REF and CG20 was investigated on additional samples. After demoulding, the specimens (cured in water) remained submerged under water until 24 h before the uniaxial compression strength test.

Table 1
Paste mixture compositions.

Mixture[a]	Quantities per specimen (40 × 40 × 160 mm^3)				
	Substitution degree	UGWM	CGWM[b]	OPC	w/b[c]
[–]	[wt.%]	[g]	[g]	[g]	[–]
REF	0	–	–	425	0.40
UG10	10	43	–	383	0.40
UG20	20	85	–	340	0.40
UG30	30	128	–	298	0.40
CG10	10	–	43	383	0.40
CG20	20	–	85	340	0.40
CG30	30	–	128	298	0.40

[a] For each curing age, three specimens of each mixture were prepared
[b] Calcination temperature of GWM = 850 °C
[c] w/b: water/binder ratio, binder equal to cement or cement and CGWM

2.2.2. Concrete mixtures

In this study, the same binder proportions as for the binder pastes, namely cement substitution rates of 10 wt%, 20 wt% and 30 wt% by UGWM respectively CGWM, were considered in the mix design of the concrete mixtures to study the characteristics in the fresh and hardened state of the investigated concretes. The volumetric mix design, as presented in Table 2, was applied to achieve concretes of class C40/50, according to DIN EN 206–1 [53]. For the concrete mixtures, the binder: aggregate (b:ag) ratio ranged around 1:3.7 and the water/binder ratio was fixed at 0,42 for all mixtures. The mixture C_REF without GWM powders was set as reference mixture. An increase of the mixture water content or the use of a superplasticiser to achieve the same consistency and workability (same slump values) was not considered in this study, as the performance of the hardened concrete, respectively the properties of the different binder matrices in the hardened composite structure were prioritised.

The mixing procedure was kept consistent for all the concrete mixtures: First of all, the fine and coarse aggregates are poured in the concrete mixer, and about two-thirds of the determined water quantity is added and briefly mixed. Then, the binder (cement only, respectively cement and GWM powder) is added and mixed for 30 s. Without interrupting the mixing process, the remaining water is poured in, followed by a mixing time of 90 s. After the mixing procedure, the consistency of all the fresh concrete mixtures was determined. All the specimen were cast in three layers, where each layer was compacted on a vibrating table until no further air bubbles appear (reduction of air voids) as prescribed by DIN EN 12390–2/A20 [54]. The samples were stored at room temperature for 24 h. After demoulding, the specimens are stored and cured under water for 7 days, then dry storage at ambient temperature is applied until 28 days of curing age. The samples tested after 56 days are submerged in water for 35 days and stored at room temperature for 21 days, according to DIN EN 12390–2/A20 [54].

2.3. Experimental methods

2.3.1. Physicochemical and mineralogical properties of the primary materials

The grain size distribution of concrete aggregates (MSG) was examined using the dry sieving method, according to EN 933–1 [55]. The particle size distributions of the powder samples OPC, UGWM and CGWM, were determined by laser diffraction technique using a particle size analyser (HELOS-RODOS-VIBRI from Sympatec GmbH). A wavelength dispersive X-ray fluorescence spectrometer (S8 TIGER from Bruker AXS GmbH) was used to detect the elemental composition of the powder samples using the XRF method. A powder X-ray diffractometer (D4 ENDEAVOR from Bruker AXS GmbH) using Cu K_α radiation was used to determine the mineralogy of the powders by X-ray diffraction analysis using the Rietveld refinement method [56].

2.3.2. Isothermal calorimetry, compressive strength test of the hardened pastes and shrinkage test

The analysis of early hydration phases of four cement pastes, namely one control mixture (cement only) and three cement pastes including CGWM powders at OPC replacement levels of 10, 20 and 30 wt%, were determined using isothermal calorimetry. The rate and the extent of the hydration heat were monitored and quantified by a thermal activity monitor (TAM, TA Instruments) as a function of time at 20.0 °C, and the mixtures were prepared at fixed w/b ratio of 0.4. Two separate measurements were performed to determine the evolution of the hydration heat for all samples: The first measurement was carried out for the first 30 min using the high sensitivity isothermal titration calorimetry [57,58], appropriate for the first rapid reactions (highly exothermic and high early hydration heat release). The second measurement was performed to monitor the heat release starting from 30 min up to 40 h by isothermal microcalorimetry [59,60]. The measured thermal energy is converted into the heat flow in mW/g and the normalised cumulative heat release in J/g.

The compressive strength of the hardened binder pastes was measured using a compression testing plant (TESTING Bluhm & Feuerherdt GmbH, Germany), conform to the standard DIN EN 196–1 [52]. The presented compression strength results represent the average values of at least three valid tests on replicate specimens at the examined curing ages. The water- and air curing of the hardened specimens was performed at constant storage conditions. Further strength-based evaluations were conducted using the compressive strength results, namely the strength activity index (SAI) [61–64] to evaluate the pozzolanicity of the GWM powders and the relative strength index (RSI), proposed by [40]. The RSI method allows determining the relative strength gain or loss of the cement pastes by taking into account the considered OPC replacement level by the GWM powder.

The unrestrained drying shrinkage test was conducted on the paste mixtures, which were cast in 40 × 40 × 160 mm^3 moulds with integrated attachment pins on both ends of the specimens. After 24 h, the specimens were demoulded and were mounted on ball-bearing rollers of the measuring unit (Fig. 1) using the attachment pins (free rotatable), assuring no obstruction for volume change in any direction (unrestrained). The conical contact tip of a digital displacement gauge (linear variable differential transformer (LVDT) displacement sensors with a measuring range of 5 mm, a resolution of 0.31 µm and an accuracy of 0.2 µm) was positioned on one side of the specimens to monitor the time-dependent volume contraction (shrinkage) by measuring the variation in the length of the specimen with time while a fixed pin horizontally constrained the other side.

Table 2
Concrete mix design.

Mixture[a]	Curing ages of 28 and 56 days; Quantities for 1 m^3 [kg/m^3]						
	Binder				Aggregates		
	Substitution degree	UGWM	CGWM[b]	OPC	Grain size (0/16 mm)	Water	w/b[c]
[–]	[wt.%]	[kg]	[kg]	[kg]	[kg]	[–]	[–]
C_REF	0	–	–	429	1200	180	0.42
C_CG10	10	–	43	386	1191	180	0.42
C_CG20	20	–	86	343	1183	180	0.42
C_CG30	30	–	129	300	1174	180	0.42
C_UG10	10	43	–	386	1191	180	0.42
C_UG20	20	86	–	343	1183	180	0.42
C_UG30	30	129	–	300	1174	180	0.42
ρ [kg/dm^3]		2.52	2.50	3.10	2.40	1.00	

[a] For the curing each curing age, three specimens of each mixture were prepared
[b] Calcination temperature of GWM = 850 °C
[c] w/b: water/binder ratio, binder equal to cement or cement and CGWM

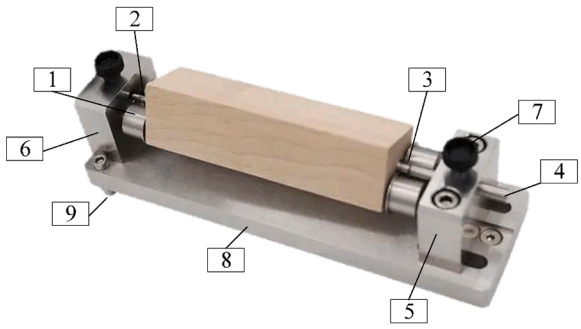

1. Ball-bearing rollers as support
2. Pin, replaced by digital displacement gauge
3. Pin, integrally cast-in or attached on both sides of specimen
4. Pin, used as horizontal constraint on one side
5. Bearing block, position adjustable
6. Bearing block, fixed
7. Locking mechanism
8.+ 9. Steel base plate, inclined position by supporting feet

Fig. 1. Setup of the shrinkage test.

2.3.3. Characteristics of fresh concrete, mechanical properties of the examined concretes, carbonation test and scanning electron microscopy (SEM) analysis

The properties of the different fresh concrete were studied by measuring their consistency at the plastic state, directly after the preparation of the mixtures by concrete slump test, according to EN12350-2 [65]. The slump value is determined as the difference in height between the level of the standardised slump cone (Abrams cone; height = 300 mm) and the height of the collapsed fresh concrete after removing the cone in which it was compacted. The mixture C_REF was assigned as reference concrete to assess the workability of the concrete mixtures containing GWM powders.

The hardened concrete properties of all concrete specimens were tested by compressive strength test on cylinders (Ø150 × 300 mm) at 28 and 56 days of curing age using a compression testing machine (TESTING Bluhm & Feuerherdt GmbH, Germany), conform to the standard EN 206 [53] and according to EN 12390-3 [66]. Additionally, the modulus of elasticity (elastic modulus) of the different hardened concrete samples was determined according to EN 12390-13 [67]. Curing of the samples was performed according to DIN EN 12390-2/A20 [54], and before the compression tests, the surface irregularities of the cylindrical specimens were polished into plane contact surfaces to ensure a uniform pressure distribution.

The carbonation of the investigated concrete mixtures is assessed at curing ages of 28 and 56 days (specimens are cured under water for 7 days, then stored at room temperature until carbonation test) by applying an indicator fluid (phenolphthalein solution) on a freshly fractured concrete surface according to EN 14630 [68]. After the application of the indicator, the resulting violet area represents the non-carbonated concrete zones, and its distance to the outer concrete shell is measured as the carbonation depth.

The microstructure was examined on broken fractions of compressed concrete specimens (including gold sputter coating to prevent charging of the specimen and for higher resolution images) using a high performing JEOL JSM 6010 analytical scanning electron microscope with integrated elemental analysis by energy-dispersive X-ray spectroscopy (EDS), which allowed to produce high-quality microstructural observations by detection of secondary electrons (SEs), backscattered electrons (BSEs) and Auger electrons (AEs) from the interaction of the primary electron beam with the investigated specimens following a raster scan pattern.

3. Results and discussions

3.1. Physicochemical properties and mineralogy of the primary materials

3.1.1. Particle size distribution of the used components

The grading curve of the mixed aggregates MSG, presented in Fig. 2, was determined by sieve analysis and the grain-size distribution of MSG was classified to the A/B16 aggregate grading range (coarse- to medium-grained) according to EN 933-1 [55]. From the particle size analysis by laser diffraction, the GWM powders show the finest particle size distribution among all the examined materials (Fig. 2). The abbreviation dX = Y indicates that X% of the particles in the sample have a diameter size of Y or smaller. UGWM shows the finest grain size range (d10-d90) from 1.47 to 41.51 µm with respective mean particle sizes (d50) of 7.22 µm, whereas, owing to the clumping effect due to the calcination process, CGWM is slightly coarser with d10-d90 ranging from 1.68 µm to 58.30 µm and d50 of 9.02 µm. The OPC powder shows a mean particle size range of 11.32 µm.

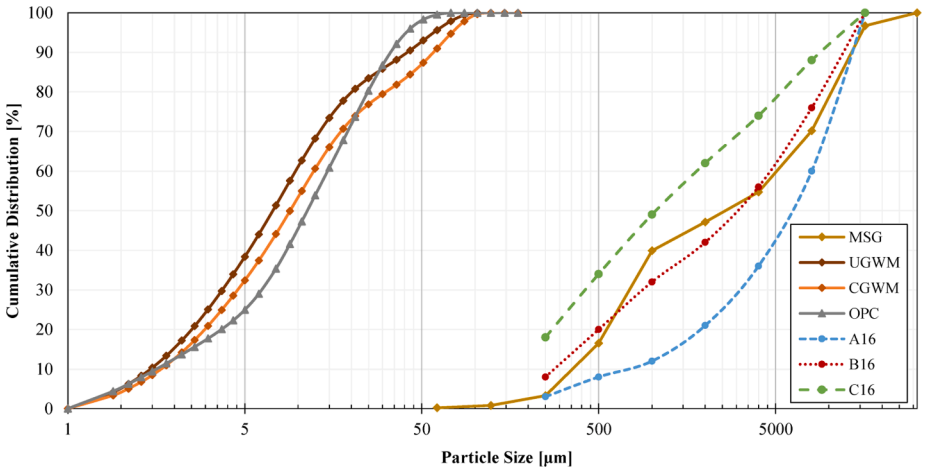

Fig. 2. Particle size distribution of all used materials. UGWM, CGWM (calcined at 850 °C), OPC powders and MSG aggregates; A/B/C 16 grading curves according to EN 933-1 [55].

3.1.2. Chemical composition and mineralogy of the applied powders

The chemical compositions of the UGWM and CGWM powders are presented in Table 3 and comply with the findings from other works [39–41] by confirming the aluminosilicate nature of the investigated materials with the primary elemental composition of SiO_2 (elevated content), Al_2O_3 and Fe_2O_3 (medium content). The chemical evaluation of OPC verifies the oxide composition of ordinary Portland cement of type CEM I 42.5 R with elevated CaO, moderate SiO_2, and minor Al_2O_3 and Fe_2O_3 contents [69,70].

The quantitative XRD analysis was carried out based on the method described in [40,71], and the mineralogical compositions of the binder constituents are summarised in Table 4. The used Ordinary Portland Cement, in addition to the traditional cement clinker phases (Alite, Belite, aluminoferrite and aluminate), revealed the presence of a hydrous calcium sulphate phase, namely anhydrite ($CaSO_4$), as well as calcite ($CaCO_3$), Portlandite ($Ca(OH)_2$), and quartz (SiO_2). The main crystalline phases identified in the GWM powders were quartz, muscovite, followed by illite and kaolinite as clay minerals, hematite and the amorphous portions.

3.2. Early hydration kinetics, long-term volumetric changes due to shrinkage and mechanical performances of the hardened blended cement pastes

3.2.1. Hydration heat flow by isothermal calorimetry

The evolution of the heat flow profiles of the plain and binary cement pastes for the first 30 min are presented in Fig. 3**a**, from 30 min up to 40 h in Fig. 3**b** and the cumulative heat release up to 40 h in Fig. 3**c**. During the initial phase of cement hydration (pre-induction period) after addition of water, the rapid dissolution of the cement minerals, C_3A (calcium aluminate) and C_3S (alite), into unstable, reactive ions in the pore solution leads to the formation of stable solid phases accompanied with exothermic heat release. As shown in Fig. 3**a**, the highest peaks of the initial hydration heat of each examined fresh pastes occurred in the first minutes after water addition and exhibited a non-monotonic progression as a slight leftward shift of the heat evolution curves of the cement pastes containing CGWM powders was observed. Furthermore, only for the cement pastes containing 10 wt% of CGWM, a representative enhancement was traceable, mainly due to its positive contribution by the initial dissolution of additional ions to the saturation of the pore solution, which was not observed for the pastes with higher contents of CGWM (oversaturation of the pore solution with aluminate and silicate ions). Following the heat profile curves, illustrated in Fig. 3**b**, no correlation between the incremental CGWM content and the heterogeneous nucleation of additional C-S-H phases could be observed as the released hydration heat declined with increasing OPC replacement levels by the CGWM powders. The decline of the hydration heat rates proportionally to the CGWM content becomes visible in Fig. 3**c** as lower slopes are observed during the acceleration period, which confirms that the higher OPC replacement levels by a slow-reacting medium-pozzolanic material like CGWM reduce the extent of hydration reaction at early ages, and the overall dilution effect, as well as the agglomeration effect between the fine aluminosilicate particles, dominate their potential to act as nucleation sites for additional hydration of the cement grains. The higher hydration rates of the REF mixture are carried over all the examined hydration stages resulting in higher cumulative heat release up to 40 h. These results regarding the evolution of the hydration heat release of the investigated cement pastes complement earlier findings [39–41] that the incorporation of higher amounts of CGWM in blended cement pastes exhibits minor to no significant physiochemical effects as the CGWM powders could provide no larger interfacial surface area for higher hydration reaction rates (C-S-H seeding) by performing as nucleation sites during the early hydration stages of the cement matrices.

3.2.2. Shrinkage behaviour of blended cement pastes

The unrestrained drying shrinkage of hardening paste mixtures was measured as the variation in length due to volume change over time at constant storage conditions. The temperature [°C] and the relative humidity [%] were recorded over the entire measurement period and ranged around 21.3 ± 1.4 °C, respectively 56.7 ± 12.0% of relative humidity (Fig. 4). The drying shrinkage behaviours of the control mixture REF and the blended cement pastes CG10, CG20 and CG30 over 80 days is plotted in Fig. 4. Overall, the drying shrinkage magnitudes of all specimens increased rapidly for the first two weeks, followed by slower increase rates in the subsequent months down to constancy. Over the whole examined time, REF exhibited the largest shrinkage values. CG10 and CG20 experienced almost identical evolution of the shrinkage values and therefore presented similar shrinkage behaviour, whereas CG30 exhibited a short swelling period in the first two days, followed by a larger shrinkage rate than REF until stabilising around the shrinkage magnitudes of CG10 and CG20 at 60 days. The expansive effects of swelling of the paste mixtures with higher CGWM contents can be related to the larger soaking of portions of mixture water by the aluminosilicate raw material, which influences the chemical and autogenous shrinkage of the cement-CGWM pastes at higher OPC replacement levels at early curing ages [72,73].

After 7 days of curing age, CG10, CG20 and CG30 experienced 18%, 23% and 15% less contraction deformations than the control mixture. The maximum shrinkage values of REF, CG10, CG20 and CG30 up 80 days were at 508.6 µm/m, 489.4 µm/m, 484.1 µm/m and 469.8 µm/m, i.e. the experienced shrinkage is 4%, 5% and 8% less for CG10, CG20 and CG30 than that of the reference mixture REF. The measured maximum shrinkage values comply within the indicative range for acceptable shrinkage deformations for standard concrete from 0.2 mm/m up to 0.6 mm/m [74]. The evaluation of the shrinkage magnitudes of the investigated pastes approves the positive enhancements of the time-dependant properties of blended cement pastes by incorporating CGWM as SCM due to the improved packing of the constituents and the formation of additional pozzolanic hydration products.

3.3. Compressive strength tests of hardened pastes

The results of the 28- and 56-day compression strength tests of the hardened pastes with different OPC replacement levels by UGWM and CGWM powders are presented in Fig. 5. The indicated values represent the mean compressive strengths out of at least three valid compression tests on replicates. For blended cement pastes containing 20 wt% and 30 wt% of GWM powders (both UGWM and CGWM), consistent gains in compressive strength from 28 days up to 56 days were considered. For REF, UG10 and CG10, a slight reduction of the compressive strength was

Table 3
Chemical composition of OPC, UGWM and CGWM powders.

Sample	Chemical composition									
	SiO_2	Al_2O_3	Fe_2O_3	CaO	MgO	SO_3	Na_2O	K_2O	TiO_2	MnO
[–]	[%]	[%]	[%]	[%]	[%]	[%]	[%]	[%]	[%]	[%]
OPC	18.94	4.68	4.25	65.56	1.22	2.91	0.21	0.52	0.33	0.34
UGWM	65.06	19.53	9.37	0.41	1.66	0.09	0.24	2.72	0.85	0.06
CGWM	64.10	20.29	8.91	0.41	1.81	0.00	0.24	3.26	0.90	0.08

Table 4
Mineralogical composition (quantitative) of OPC, UGWM and CGWM powders.

Sample	Mineralogical composition [%]							
	C_3S	C_2S	C_4AF	C_3A	Anhydrite	Calcite	Portlandite	Quartz
OPC	52.2	24.6	11.8	1.7	2.6	4.8	1.8	0.5
	Quartz[a]	Muscovite	Illite	Kaolinite	Hematite	$KAl_3Si_3O_{11}$	Amorph	
UGWM[b]	35.0	16.5	13.2	11.3	0.6	1.5	21.9	
CGWM[b]	35.0	8.7	12.4	0.3	2.1	7.2	34.4	

[a] Quartz content fixed for normalisation of data; [b] Quantitative XRD data from[40]

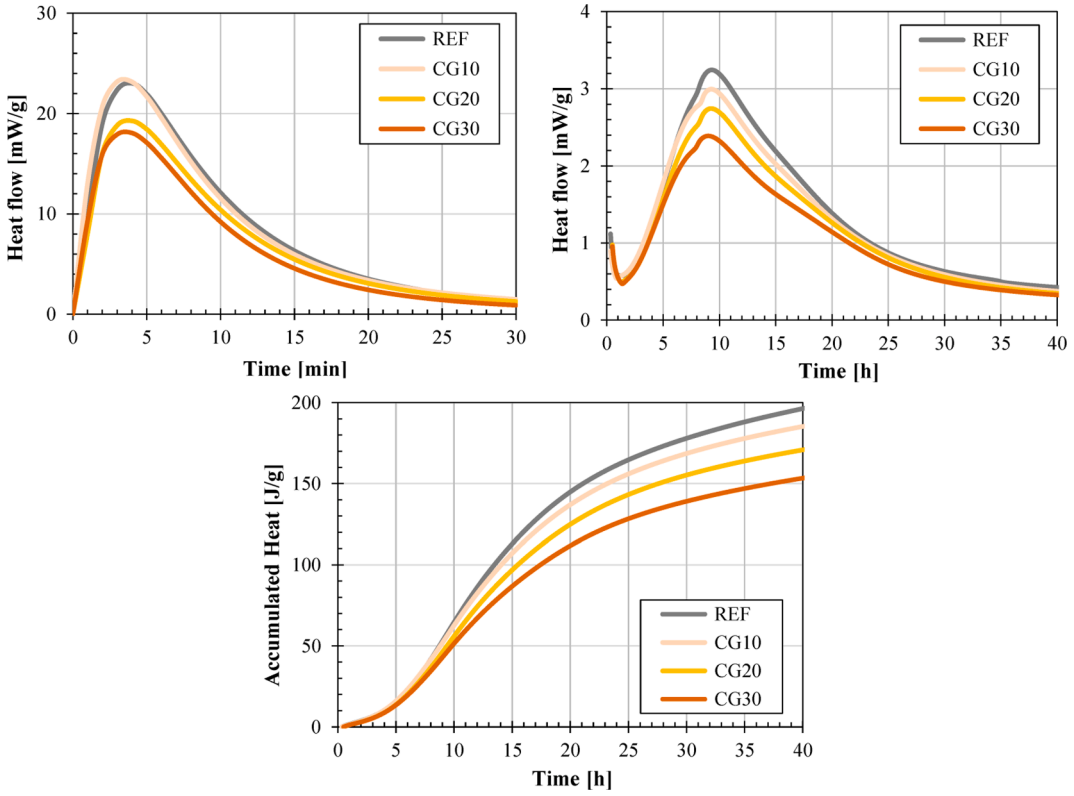

Fig. 3. Isothermal calorimetric curves of REF, CG10, CG20 and CG30. a) heat flow from up to 30 min, b) heat flow from 30 min up to 40 h, c) accumulated heat release up to 40 h.

observed from 28 days to 56 days.

Overall, the cement pastes containing GWM powders reached lower compressive strengths than the control mixture over the entire examined curing ages. At 28 days, the lower pozzolanicity of the UGWM powders compared to CGWM powders becomes evident as for same mixture proportions, lower compressive strengths are achieved by the hardened pastes containing UGWM at OPC replacement levels of 20 wt% and 30 wt%. The lower reactivity of UGWM becomes more significant with increasing curing age, as at 56 days, the compressive strengths of hardened pastes incorporating UGWM powders decrease with higher substitution degrees of OPC, whereas the mechanical performances of hardened pastes containing CGWM increase slightly with higher OPC replacement levels. This representative trend indicates the formation of additional hydration products due to pozzolanic reactions between the CGWM powders and unreacted calcium hydroxide (Portlandite), the main co-products from the hydration of cement clinker minerals. The SAI method (Fig. 6**a**) and the RSI method (Fig. 6**b**) were applied to assess the pozzolanic reactivity of UGWM and CGWM as potential OPC substitutes. According to ASTM C311 [75], the strength activity indices for hardened cement pastes are calculated for OPC replacement levels of 20 wt% and the 75% minimum threshold according to ASTM C618 [76] represents the minimal SAI requirement on calcined pozzolans after 28 days of curing age. As shown in Fig. 6**a**, the computed SAI of UG20 does not fulfil the minimal requirement at 28 days of curing and indicates that the incorporation of the UGWM powder rather contributes to a dilution effect at higher OPC replacement levels which instead builds a physical constraint for the clinker hydration reactions than an improvement due to measurable pozzolanicity.

In comparison, the SAI of CG20 at 28 days of curing age surpasses the minimal requirement by 13.1% and thereby confirms that the tested pozzolan, namely CGWM powder, can be considered as SCM [39–41] as it sufficiently contributes to the development of the required minimal strengths in an OPC-based mixture. As the SAI method, according to [76], is an indicative assessment method and does not evaluate the optimal substitution degree, the indices are computed for all hardened cement paste specimens at all curing ages. It can be observed that the hardened pastes containing UGWM powders fulfil the minimal threshold at later curing ages, as the development of additional calcium silicate hydrate (C-S-H) products due to later pozzolanic reactions becomes more significant.

The evaluation of the computed relative strength indices illustrated in Fig. 6**b** confirms the previous statements from the comparative analysis of the absolute compression strength values as well as the SAI analysis. The assessment of the RSI verifies the positive contributions of

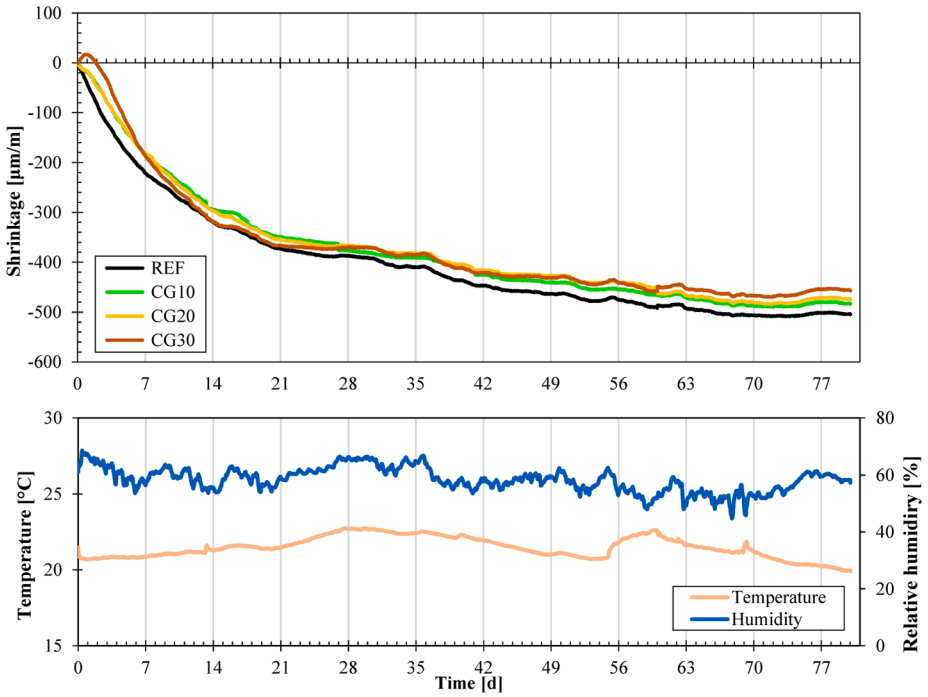

Fig. 4. Evolution of shrinkage of the hardened paste mixtures REF, CG10, CG20 and CG30, including the development of relative humidity [%] and temperature [°C] up to 80 days.

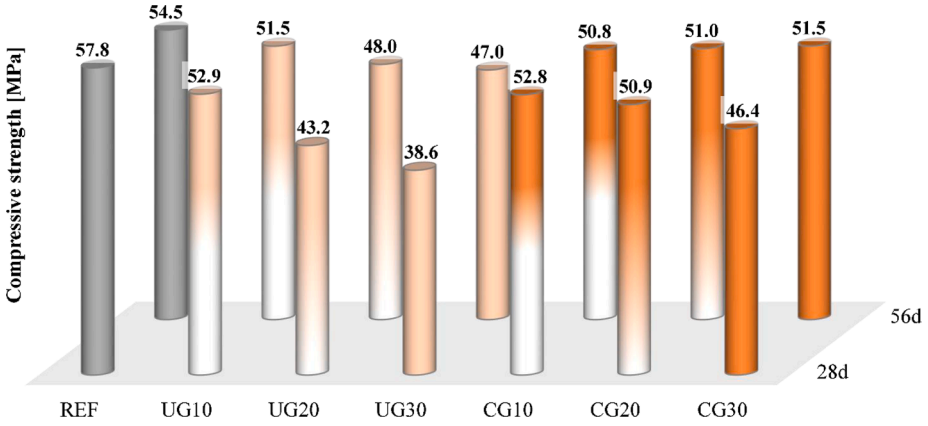

Fig. 5. Evolution of the mechanical properties of hardened pastes of seven different paste mixtures, namely REF, UG10, UG20, UG30, CG10, CG20 and CG30 at 28 and 56 days of curing age.

UG10 and CG10 for all investigated curing ages, which suggest that for OPC replacement level of 10 wt%, the physical filler effect of the GWM powders is rather predominant than the chemical contributions to the mechanical performances. Additionally, the negative contributions by relative strength loss of UG20 and UG30 at 28 days of curing age are also confirmed by the RSIs. Furthermore, positive relative strength gains up to 56 days of curing age for the hardened cement pastes using higher OPC substitution degrees of 20 wt% and 30 wt% by UGWM and CGWM are observed.

Fig. 7 illustrates the evolution of compressive strength results of hardened pastes of REF, UG20 and CG20 at 1, 3, 7, 28, 56 and 90 days (cured in air), and the strength development of REF and CG20 at 7, 28, 56 and 90 days (cured in water). By comparison of the mechanical performances of air-cured and water-cured specimens of the same mixing proportions, it can be concluded that the investigated specimens did not reveal any significant dissimilarities in terms of mechanical strength due to applied curing conditions [77], except for CG20 at 90 days. A gain of 10% in compressive strength was observed for CG20_W compared to CG20 at 90 days, which can be explained by the continuous hydration of belite (C_2S) in water curing conditions at later ages [77], leading to the formation of calcium hydroxide (CH), which undergoes into a pozzolanic reaction with available CGWM to form additional hydration products. Furthermore, for the paste mixture REF, a representative decline in compressive strength was observed after 28 days of curing age in both examined curing conditions. The exact reason for the drop in strength is still unclear, but a possible explanation could be the applied high w/b ratio leading to larger volumetric shrinkage strains (drying shrinkage) in combination with proceeding carbonation reactions of the cement matrix with the presence of unreacted CH at increasing curing age, leading to the deterioration of specimens (cracks). This trend was not visible for all the blended cement paste mixtures containing UGWM and CGWM at any substitution degree, as the excess CH at later curing ages is consumed by the pozzolanic reaction with the examined SCM.

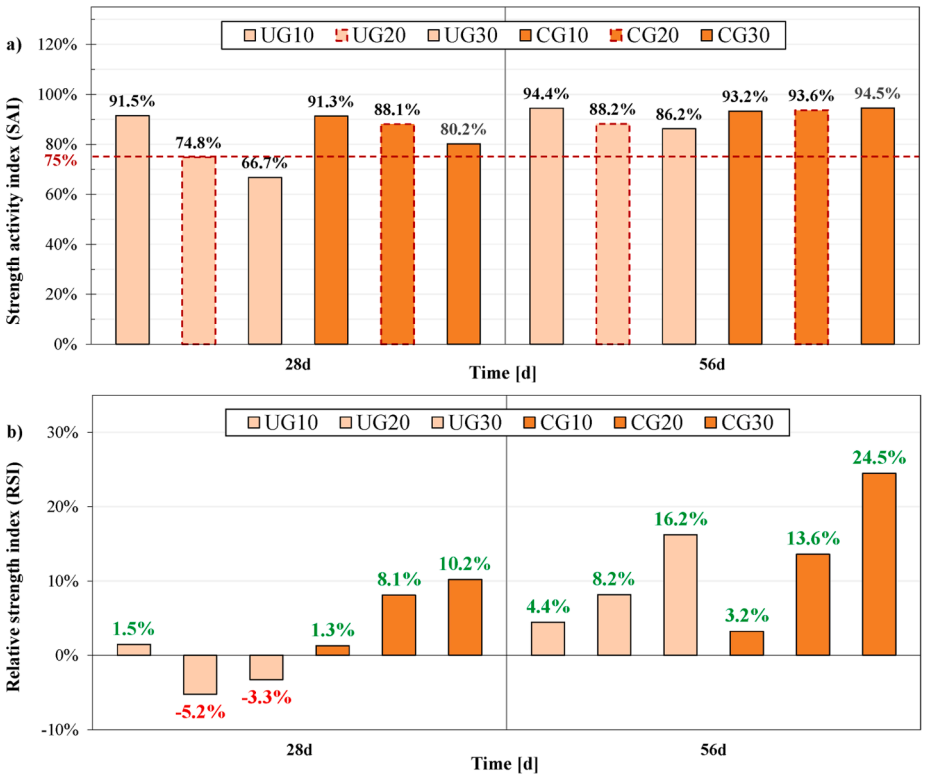

Fig. 6. Strength-based evaluations. a) Strength activity index (SAI; dashed line represents the limit for pozzolanic activity and highlights the considered mixtures according to ASTM C618 [76]) and b) relative strength index (RSI) [40].

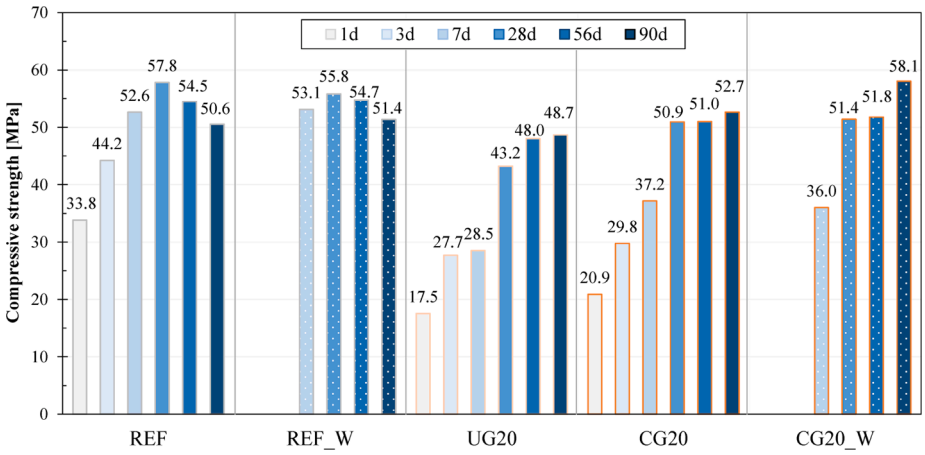

Fig. 7. Evolution of the mechanical properties of hardened pastes from three different paste mixtures: REF, UG20 and CG20 (cured in the air), REF_W and CG20_W (cured in water) at 1, 3, 7, 28, 56 and 90 days of curing age (strength tests after 1 day and 3 days skipped for water cured specimens).

3.4. Fresh concrete properties, compressive strength, carbonation test and SEM analysis of the investigated concrete mixtures

3.4.1. Properties of fresh concrete, the evolution of mechanical properties of the hardened concrete specimens and depth of carbonation

As the following results present the performances of the first trials, the use of superplasticizer was excluded (avoid segregation effects due to inadequate dosage) by assuring a homogenous compaction of the fresh concrete (vibration table) to understand the "real effects" of the incorporation of GWM powders on the concrete mixes in the fresh and hardened state. The results of the slump test are given in Table 5. From the evaluation of these results, it is confirmed that higher GWM powder content in the concrete mixes influences the fresh concrete properties as a significant reduction of the workability of concrete was observed. The major contribution to the reduction of the degree of workability with higher GWM powder contents can be attributed to the fineness (higher surface area [40,41]) of the aluminosilicate particles. Although overall, homogenous compaction of the fresh concrete was possible by vibration, these results are in agreement with the findings from the literature [78–80] and suggest the usage of adequate dosage of superplasticisers to improve the flowability of concretes incorporating higher portions of SCMs (GWM powders) and, thereby, adapt the workability of the concretes for various constructive applications.

The properties and the evolution of the compressive strengths of the examined concrete mixtures after 28 days and 56 days are given in Table 5 and illustrated in Fig. 8, and the findings confirm that the incorporation of the different GWM powders influences the characteristics and the compressive strength of the binary blended concrete

Table 5
Measured parameters and results of the strength tests of the examined concrete mixtures.

Sample	Slump	ρ_{28}	$f_{cyl,28}$	$\Delta f_{cyl,REF}$	$E_{c,28}$	ρ_{56}	$f_{cyl,56}$	$\Delta f_{cyl,REF}$	$E_{c,56}$	Cd_{28}	Cd_{56}
	[mm]	[kg/dm^3]	[MPa]	[%]	[GPa]	[kg/dm^3]	[MPa]	[%]	[GPa]	[mm]	[mm]
C_REF	215.0	2.29	39.3	–	29.47	2.29	46.0	–	28.79	1.25	2.75
C_UG10	110.0	2.29	41.1	4.6%	29.45	2.29	46.5	1.21%	28.18	0.75	1.75
C_UG20	55.0	2.18	29.7	−24.5%	21.62	2.19	34.8	−24.31%	20.95	1.75	3.00
C_UG30	42.5	2.17	25.6	−34.8%	19.49	2.20	31.7	−31.05%	21.50	2.50	3.25
C_CG10	165.0	2.27	38.7	−1.6%	26.91	2.26	44.6	−2.96%	26.95	0.50	1.75
C_CG20	60.5	2.25	38.8	−1.3%	25.61	2.27	45.4	−1.30%	28.42	1.25	2.50
C_CG30	48.0	2.25	33.6	−14.5%	24.82	2.23	38.7	−15.92%	25.78	1.75	2.75

ρ_X – bulk density of concrete at X days of curing age
$f_{cyl,X}$ - compressive strength of concrete cylinder after X days
$E_{c,X}$ - elastic modulus of concrete at X days of curing age
Cd_X - carbonation depth after X days
$\Delta f_{cyl,REF}$ - difference of compressive strength between two curing ages or compared to the reference mixture

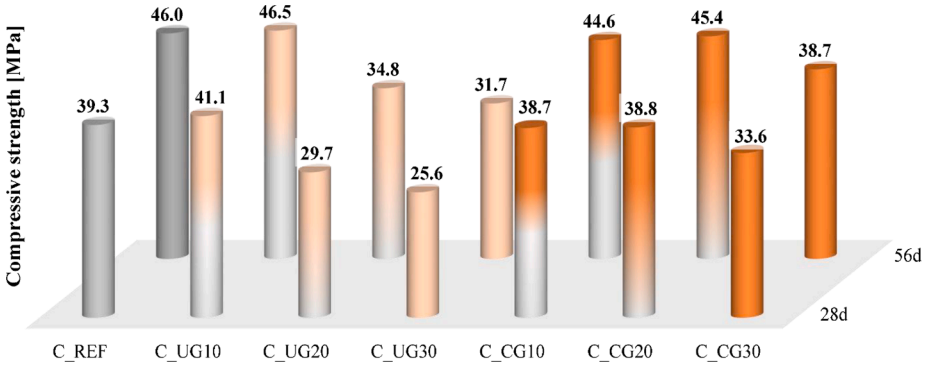

Fig. 8. Evolution of the compressive strength of the examined concrete mixtures, namely C_REF, C_UG10, C_UG20, C_UG30, C_CG10, C_CG20 and C_CG30 at 28 and 56 days of curing age.

mixes. For all the investigated concrete mixes, the compressive strength increased with growing curing age, ranging from 25.6 MPa to 41.1 MPa after 28 days up to from 31.7 MPa to 46.5 MPa after 56 days. Moreover, longer water immersion of the concrete samples led to a steady increase in compressive strength, confirming the hydraulic behaviour of the binder pastes. The binary concrete mixes C_UG10, C_CG10 and C_CG20 achieved the highest compressive strengths comparable to OPC concrete at around 40 MPa after 28 days and around 46 MPa after 56 days. At all examined curing ages, C_UG10 slightly exceeded the target compressive strength of the reference mixture, mainly due to the better packing of the constituents (filler effect) by the formation of a denser aggregate-blended cement paste matrix. Furthermore, the incorporation of higher portions of UGWM powders are revealed to have detrimental effects on the mechanical properties of blended concretes as the low reactivity of the UGWM powder hinders effectivity of pozzolanic reaction with the free Portlandite and rather build a physical obstruction to the hydration process (dilution effect). The development of elastic modulus (E_c) and the measured densities (ρ) of the different concrete mixes reflect and comply with the evolution of their mechanical strengths by producing lower values for concrete mixes with higher UGWM powder contents and comparable values to the reference mixture for C_UG10, C_CG10 and C_CG20.

The resulting mechanical parameters of the examined concrete mixes confirm the findings from the strength assessments on the hardened blended cement pastes and implicate that the incorporation of UGWM powders at OPC replacement levels of 10 wt%, and CGWM powders at OPC replacement levels of 10 wt% and 20 wt% in binary concrete mixes can be considered as viable and competitive proportions for alternative SCM-based concretes for various constructive applications without compromising on the concrete's mechanical performance.

The results of the measurement of the carbonation depths (Cd) of the investigated concrete samples after 28 days and 56 days are presented in Table 5. Fig. 9 shows the cross-sections of the investigated specimens after application of the phenolphthalein indicator solution after 56 days. The comparison of the carbonation depths of the concretes after 28 days reveals that at early curing ages the overall measured level of carbonation is very low (around 1 mm) as the hydration reactions are progressing and the interstices are being filled with hydration products to increase the strength development further. However, C_UG10, C_CG10 and C_CG20 already express lower or equal carbonation depths than the reference mixture C_REF. This positive enhancement can be explained by finer pore structure (denser packing of binder particles and additional hydration products) and the early pozzolanic reaction of available free $Ca(OH)_2$ with reactive CGWM powders. Whereas, for concretes with higher GWM powder contents, greater rates and depths of carbonation compared to the reference concrete C_REF were measured due to lower reactivity of UGWM in combination with the predominant dilution effect (less OPC available in the mixture) at early curing ages. Beyond that, at any examined time of exposure, the advancement of carbonation of the binary blended concretes incorporating 10 wt% and 20 wt% of CGWM were lower than in C_REF.

3.4.2. *Microstructural analysis by SEM*

A selection of micrographs of broken fractions of all the investigated concrete mixtures are presented in Fig. 10, Fig. 11 and Fig. 12, which were produced by SEM analysis with verification using elemental analysis by EDS. Fig. 10 illustrates the microstructural features of the reference concrete C_REF. In Fig. 10**a**, the development of a compact microstructure of hardened cement paste with dense and homogenous coverage of the quartz particles can be observed, whereas Fig. 10**b** shows a well-formed framework of needle-like and amorphous C-S-H mineral formations of the same concrete mixture. Fig. 11 depicts a

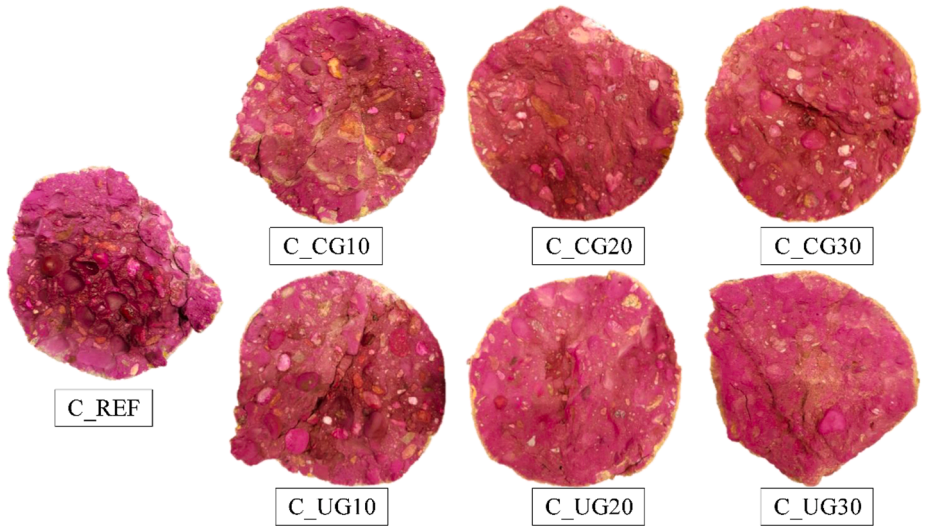

Fig. 9. Carbonation depth test on cross-sections of C_REF, C_UG10, C_UG20, C_UG30, C_CG10, C_CG20 and C_CG30 after 56 days.

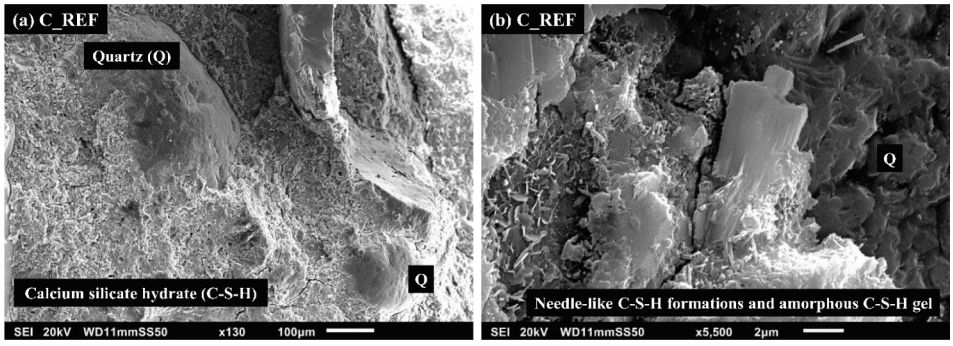

Fig. 10. SEM micrographs of C_REF: a) quartz (Q) particles covered by compact hardened cement paste (x130); b) needle-like and amorphous calcium silicate hydrate (C-S-H) phases (x5500).

compilation of micrographs showing the microscale morphology of the concrete mixtures containing UGWM powders at varying OPC substitution degrees. In Fig. 11**a** and Fig. 11**b, a** dense microstructure of C_UG10, consisting of mainly calcium silicate hydrate phases without any traces of unmixed or unreacted aluminosilicate particles, was detected; additionally, at the interfacial transition zones between the cement matrix and the aggregates, extensive developments of needle-like, fibrillar and amorphous hydration products were localised, which explain the enhanced performances compared to the control mixture by an improved bond between the hydrous and amorphous cementitious formations and the concrete aggregates. Fig. 11**c**, **d** and **e** show the microstructural compositions of C_UG20, consisting of amorphous compounds with semi-reacted Portlandite crystals (CH), large aluminosilicate crystals covered by cementitious and pozzolanic hydration products and dispersed areas of unmixed, semi-mixed and unreacted aluminosilicate particles (UGWM) surrounded by amorphous cementitious formations, which suggests that some unreacted CH could not be bound by the low-reactive aluminosilicate particles of UGWM to form additional pozzolanic hydration products and thereby explain the decline of mechanical performance of concrete mixtures with higher UGWM proportions. The microstructure of C_UG30 (Fig. 11**f**) reflects and explains the detrimental effect of higher UGWM contents in concrete mixtures on the resulting mechanical performances as larger entrapped air voids and micropores, as well as dispersed locations of unmixed or unreacted GWM powders, were detected across the investigated samples. This development also suggests that higher content of UGWM, resp. CGWM is not recommended to avoid larger proportions of unmixed/semi-mixed aluminosilicate or cementitious agglomerates (dilution effect). Fig. 12 presents the microstructure of broken fractions of concrete specimens incorporating CGWM powders at varying OPC replacement levels. Similar to C_UG10, the SEM micrograph of C_UG10 (Fig. 12**a**) depicts a densely interlocked amorphous microstructure with no traceable semi-mixed or unreacted aluminosilicate particles. In Fig. 12**b** and **c**, the formation of dense microstructural networks of calcium silicate hydrates and calcium aluminosilicate hydrates covering local quartz particles and the formation of needle-like and fibrillar C-S-H phases, and pozzolanic hydration products are identified. Fig. 12**d** shows a spot of densely packed unreacted and semi-mixed aluminosilicate agglomerates. The SEM analysis of the different samples confirms a well-developed and dense microstructure of the examined binary blended concretes with extensive formations of pozzolanic hydration products and the cementitious hydration products.

4. Conclusions

The work presents the results of investigations performed on blended cement pastes and concrete mixtures incorporating processed GWM powders (originating from quarry waste sludge) as potential alternative SCMs at varying OPC replacement levels from 10 wt% up to 30 wt%. From the key findings of the different examinations, the following can be drawn:

- The physicochemical characteristics and the mineralogy of the processed raw material, CGWM powder, originating from quarry waste

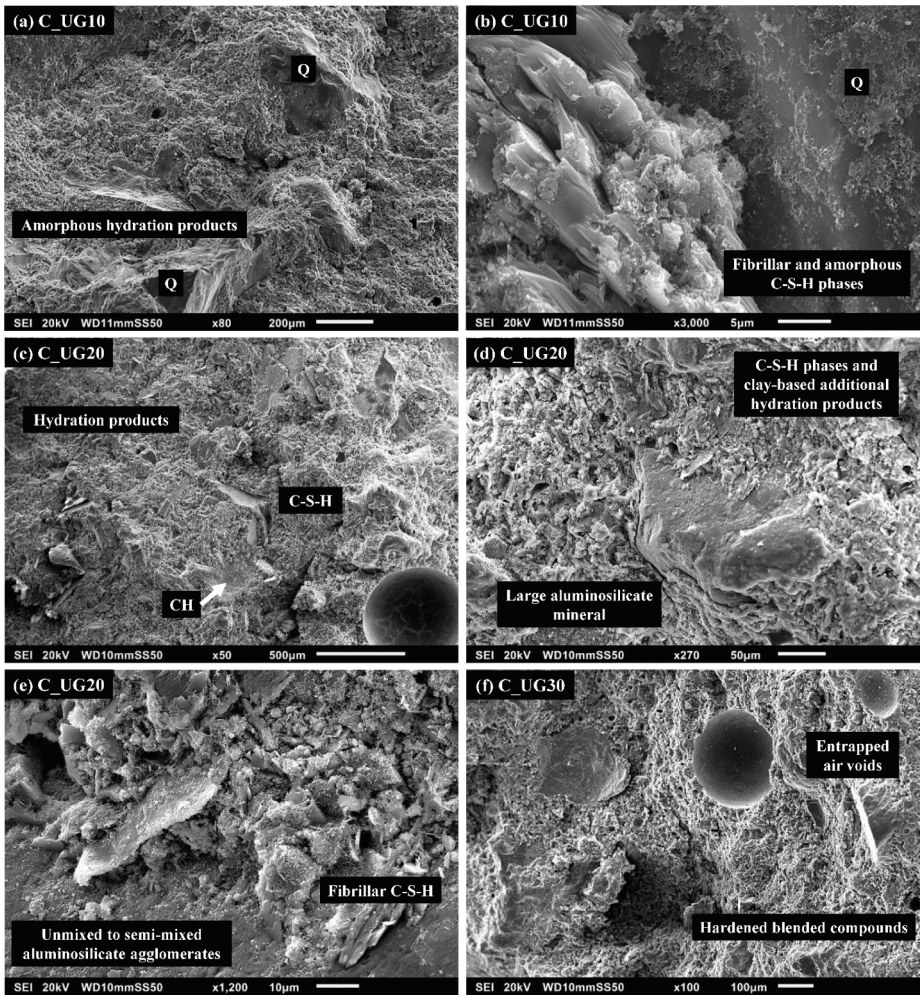

Fig. 11. SEM micrographs of C_UG10, C_UG20 and C_UG30**.** a) Hardened amorphous blended paste with dense coverage of quartz particles (x80); b) Transition zone between large quartz grain and calcium silicate hydrate (C-S-H) phases (x3000); c) Amorphous compound with semi-reacted Portlandite (CH) (x50); d) Large aluminosilicate mineral covered by compact compound consisting of cementitious and pozzolanic hydration products (x270); e) unmixed, semi-mixed and aluminosilicate particles (UGWM) were discovered surrounded by fibrillar C-S-H phases (x1200); f) irregular hardened blended cement paste with distributed large air voids (x100).

sludge, exhibits medium-reactive pozzolanic behaviour and can be considered as an alternative SCM.

- The assessment of the hydration heat release of the blended cement pastes confirms that, at the early hydration stages, the incorporation of CGWM powders exhibits minor to no significant physiochemical effects and therefore does not actively contribute to the acceleration of the early hydration reaction by acting as nucleation sites of the cement matrices.
- The drying shrinkage magnitudes of the blended cement pastes containing CGWM powders as SCM are lower over the examined period of 80 days compared to the control mixture REF. The enhancement potential of the time-dependant properties of the blended cement pastes results from the improved packing of the constituents and the formation of additional pozzolanic hydration products, which induced a reduction of about 4–8% of dry shrinkage values compared to REF.
- The GWM powders show a significant impact on the fresh concrete properties of the blended concrete mixes by greater reduction of the workability of the fresh compounds with increasing GWM powder content and therefore suggest the usage of an appropriate superplasticiser to meet the flowability requirement on fresh concrete depending on desired applications.
- The assessment of the mechanical properties of the different concrete mixes implicates that the contents of UGWM powders at OPC replacement levels of 10 wt%, and CGWM powders at OPC replacement levels of 10 wt% and 20 wt% in binary concrete mixes can be considered as viable and competitive proportions for alternative SCM-based concretes.
- For the examined time until 56 days of curing age, greater progress of carbonation was recorded for binary blended concrete using higher OPC substitution degrees by UGWM powders, whereas the advancement of carbonation of the binary blended concretes incorporating 10 wt% and 20 wt% of CGWM powders were lower compared to the reference concrete C_REF.
- The microstructural analysis of the different samples shows a firmly adhered and dense microstructural compositions of the investigated specimens, mainly consisting of extensive formations of co-existing aluminosilicate-based pozzolanic hydration products and the clinker-based hydration products.

The usage of CGWM powders in binary blended concretes can contribute to cost-savings in the manufacture of constructive elements (derived of unused quarry waste), the reduction of the environmental impacts of the cement industry as well as the great potential to the enhancement of the durability performances of the final concrete products. Further studies are required to evaluate the challenges and opportunities inherent in the GWM-based concrete products, namely the transition to large-scale processes of the used treatment activity, the improvement of the rheology, the investigations on the durability performance against concrete degradation effects, and the economic and environmental assessment of the proposed technology at industrial scale.

CRediT authorship contribution statement

Vishojit Thapa: Conceptualization, Methodology, Investigation,

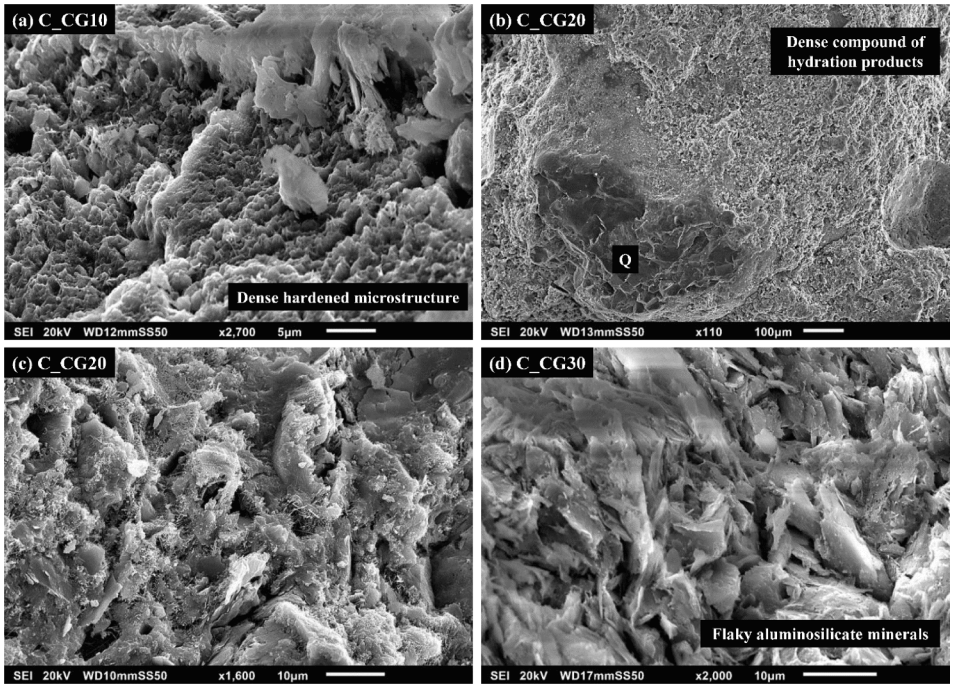

Fig. 12. SEM micrographs of C_CG10, C_CG20 and C_CG30: a) Dense amorphous structure consisting of cementitious and pozzolanic hydration products (×2700); b) compact microstructure of calcium silicate hydrates and calcium aluminosilicate hydrates covering local quartz particles (×110); c) needle-like and fibrillar C-S-H phases and pozzolanic hydration products (×1600); d) Unreacted and semi-mixed aluminosilicate agglomerates (×2000).

Resources, Formal analysis, Validation, Writing - original draft. **Danièle Waldmann:** Conceptualization, Methodology, Investigation, Resources, Supervision, Project administration, Funding acquisition, Writing - review & editing.

Declaration of Competing Interest

The authors declare that they have no known competing financial interests or personal relationships that could have appeared to influence the work reported in this paper.

Acknowledgements

The authors wish to acknowledge Carrières Feidt S.A for providing the gravel wash mud (GWM). The authors would like to express their sincere gratitude to Dr. Claude Simon from Cimalux S.A., Dr. Marcus Paul and Astrid Becker from the Wilhelm Dyckerhoff Institut (WDI) for their valuable contributions to the applied characterisation techniques, and Zornitza Tosheva from the Department of Physics and Materials Science at the University of Luxembourg for providing support to the scanning electron microscopy.

References

[1] International Energy Agency (IEA), Technology Roadmap - Low-Carbon Transition in the Cement Industry, 2018. https://www.iea.org/reports/technology-roadmap-low-carbon-transition-in-the-cement-industry.
[2] M. Gimenez, CO2 uses in the cement industry, Carbon Capture Util. Storage - SETIS. (2016) 34–35, https://doi.org/10.1007/978-3-030-30908-4_5.
[3] WBCSD Cement Sustainability Initiative, Getting the Numbers Right - GCCA in NumbeRs, GNR Proj. Report. CO2. (2017). https://www.wbcsdcement.org/index.html (accessed April 3, 2020).
[4] International Energy Agency (IEA), Cement, IEA, Paris. (2020). https://www.iea.org/reports/cement (accessed August 30, 2020).
[5] US Geological Survey, Cement Production Globally and in The U.S. from 2010 to 2019 (in Million Metric Tons), Stat. Inc. (2020). https://www-statista-com.proxy.bnl.lu/statistics/219343/cement-production-worldwide/ (accessed August 30, 2020).
[6] Global Cement Magazine, Cement production worldwide from 1995 to 2019 (in billion tons), Stat. Inc. (2019). https://www-statista-com.proxy.bnl.lu/statistics/1087115/global-cement-production-volume/ (accessed August 30, 2020).
[7] F. Pacheco-Torgal, S. Jalali, J. Labrincha, V.M. John, Eco-Efficient Concrete, Woodhead Publishing Limited, 2013.
[8] M. Thomas, Supplementary Cementing Materials in Concrete, CRC Press - Taylor & Francis Group, 2013.
[9] P. Hewlett, M. Liska, Lea's Chemistry of Cement and Concrete, Butterworth-Heinemann, 2019.
[10] EN 197-1:2011, Cement - Part 1: Composition, specifications and conformity criteria for common cements, European Committee for standardization, 2011.
[11] NF EN 206/CN, Concrete - Specification, performance, production and conformity - National addition to the standard NF EN 206, AFNOR, 2014.
[12] NF P18-513:2012-08-01, Addition for concrete - Metakaolin - Specifications and conformity criteria, AFNOR, 2012.
[13] E. Özbay, M. Erdemir, H.I. Durmus, Utilization and efficiency of ground granulated blast furnace slag on concrete properties – a review, Constr. Build. Mater. 105 (2016) 423–434, https://doi.org/10.1016/j.conbuildmat.2015.12.153.
[14] M.C.G. Juenger, R. Siddique, Recent advances in understanding the role of supplementary cementitious materials in concrete, Cem. Concr. Res. cli (2015) 71–80, https://doi.org/10.1016/j.cemconres.2015.03.018.
[15] P. Suraneni, J. Weiss, Examining the pozzolanicity of supplementary cementitious materials using isothermal calorimetry and thermogravimetric analysis, Cem. Concr. Compos. 83 (2017) 273–278, https://doi.org/10.1016/j.cemconcomp.2017.07.009.
[16] S. Tongbo, W. Bin, Z. Lijun, C. Zhifeng, Meta-kaolin for high performance concrete, RILEM Bookseries. 10 (2015), https://doi.org/10.1007/978-94-017-9939-3_58.
[17] Z. Shi, M.R. Geiker, K. De Weerdt, B. Lothenbach, J. Kaufmann, W. Kunther, S. Ferreiro, D. Herfort, J. Skibsted, Durability of portland cement blends including calcined clay and limestone: interactions with sulfate, chloride and carbonate ions, RILEM Bookseries 10 (2015) 133–141, https://doi.org/10.1007/978-94-017-9939-3_17.
[18] W. Huang, H. Kazemi-Kamyab, W. Sun, K. Scrivener, Effect of replacement of silica fume with calcined clay on the hydration and microstructural development of eco-UHPFRC, Mater. Des. 121 (2017) 36–46, https://doi.org/10.1016/j.matdes.2017.02.052.
[19] R. Walker, S. Pavía, Physical properties and reactivity of pozzolans, and their influence on the properties of lime-pozzolan pastes, Mater. Struct. 44 (6) (2011) 1139–1150, https://doi.org/10.1617/s11527-010-9689-2.
[20] K. Scrivener, Calcined Clays for Sustainable Concrete, 2018. doi:10.1007/978-94-024-1207-9.
[21] R. Gmür, K.C. Thienel, N. Beuntner, Influence of aging conditions upon the properties of calcined clay and its performance as supplementary cementitious material, Cem. Concr. Compos. 72 (2016) 114–124, https://doi.org/10.1016/j.cemconcomp.2016.05.020.
[22] A. Vimmrová, M. Keppert, O. Michalko, R. Černý, Calcined gypsum-lime-metakaolin binders: Design of optimal composition, Cem. Concr. Compos. 52 (2014) 91–96, https://doi.org/10.1016/j.cemconcomp.2014.05.011.

[23] P. He, M. Wang, S. Fu, D. Jia, S. Yan, J. Yuan, J. Xu, P. Wang, Y. Zhou, Effects of Si/Al ratio on the structure and properties of metakaolin based geopolymer, Ceram. Int. 42 (13) (2016) 14416–14422, https://doi.org/10.1016/j.ceramint.2016.06.033.
[24] V.M. Malhotra, P.K. Mehta, Pozzolanic and Cementitious Materials, 1996.
[25] A. Wardhono, D.W. Law, A. Strano, The strength of alkali-activated slag/fly ash mortar blends at ambient temperature, Procedia Eng. 125 (2015) 650–656, https://doi.org/10.1016/j.proeng.2015.11.095.
[26] Y. Farnam, B. Zhang, J. Weiss, Evaluating the use of supplementary cementitious materials to mitigate damage in cementitious materials exposed to calcium chloride deicing salt, Cem. Concr. Compos. 81 (2017) 77–86, https://doi.org/10.1016/j.cemconcomp.2017.05.003.
[27] D. Nied, M. Zajac, M. Ben Haha, C. Stabler, Assessing the Synergistic Effect Between Limestone and Metakaolin and Novel Methodology to Assess the Reactivity of Calcined Clays Composite Cements based on Limestone and Metakaolin, (2015).
[28] F. Avet, E. Boehm-Courjault, K. Scrivener, Investigation of C-A-S-H composition, morphology and density in Limestone Calcined Clay Cement (LC3), Cem. Concr. Res. 115 (2019) 70–79, https://doi.org/10.1016/j.cemconres.2018.10.011.
[29] I. Mehdipour, A. Kumar, K.H. Khayat, Rheology, hydration, and strength evolution of interground limestone cement containing PCE dispersant and high volume supplementary cementitious materials, Mater. Des. 127 (2017) 54–66, https://doi.org/10.1016/j.matdes.2017.04.061.
[30] M.I. Sánchez de Rojas, J. Rivera, M. Frías, Influence of the microsilica state on pozzolanic reaction rate, Cem. Concr. Res. 29 (6) (1999) 945–949, https://doi.org/10.1016/S0008-8846(99)00085-X.
[31] M. Frías, M.I. Sánchez De Rojas, Microstructural alterations in fly ash mortars: study on phenomena affecting particle and pore size, Cem. Concr. Res. 27 (1997) 619–628, https://doi.org/10.1016/S0008-8846(97)00026-4.
[32] R. Siddique, in: Waste Materials and By-Products in Concrete, Springer, Berlin, Heidelberg, 2008, https://doi.org/10.1007/978-3-540-74294-4.
[33] B. Lothenbach, K. Scrivener, R.D. Hooton, Supplementary cementitious materials, Cem. Concr. Res. 41 (12) (2011) 1244–1256, https://doi.org/10.1016/j.cemconres.2010.12.001.
[34] W.-Y. Kuo, J.-S. Huang, T.-E. Tan, Organo-modified reservoir sludge as fine aggregates in cement mortars, Constr. Build. Mater. 21 (3) (2007) 609–615, https://doi.org/10.1016/j.conbuildmat.2005.12.009.
[35] Ł. Kotwica, W. Pichór, E. Kapeluszna, A. Różycka, Utilization of waste expanded perlite as new effective supplementary cementitious material, J. Clean. Prod. 140 (2017) 1344–1352, https://doi.org/10.1016/j.jclepro.2016.10.018.
[36] H. Lee, A. Hanif, M. Usman, J. Sim, H. Oh, Performance evaluation of concrete incorporating glass powder and glass sludge wastes as supplementary cementing material, J. Clean. Prod. 170 (2018) 683–693, https://doi.org/10.1016/j.jclepro.2017.09.133.
[37] G. Medina, I.F. Sáez del Bosque, M. Frías, M.I. Sánchez de Rojas, C. Medina, Granite quarry waste as a future eco-efficient supplementary cementitious material (SCM): Scientific and technical considerations, J. Clean. Prod. 148 (2017) 467–476, https://doi.org/10.1016/j.jclepro.2017.02.048.
[38] R.A. Schankoski, P.R. de Matos, R. Pilar, L.R. Prudêncio, R.D. Ferron, Rheological properties and surface finish quality of eco-friendly self-compacting concretes containing quarry waste powders, J. Clean. Prod. 257 (2020) 120508, https://doi.org/10.1016/j.jclepro.2020.120508.
[39] V.B. Thapa, D. Waldmann, J.-F. Wagner, A. Lecomte, Assessment of the suitability of gravel wash mud as raw material for the synthesis of an alkali-activated binder, Appl. Clay Sci. 161 (2018) 110–118, https://doi.org/10.1016/j.clay.2018.04.025.
[40] V.B. Thapa, D. Waldmann, C. Simon, Gravel wash mud, a quarry waste material as supplementary cementitious material (SCM), Cem. Concr. Res. 124 (2019) 105833, https://doi.org/10.1016/j.cemconres.2019.105833.
[41] V.B. Thapa, D. Waldmann, Performance of lime-metakaolin pastes using gravel wash mud (GWM), Cem. Concr. Compos. 114 (2020) 103772, https://doi.org/10.1016/j.cemconcomp.2020.103772.
[42] E. Cohen, A. Peled, G. Bar-Nes, Dolomite-based quarry-dust as a substitute for fly-ash geopolymers and cement pastes, J. Clean. Prod. 235 (2019) 910–919, https://doi.org/10.1016/j.jclepro.2019.06.261.
[43] S. Krishnan, S.K. Kanaujia, S. Mithia, S. Bishnoi, Hydration kinetics and mechanisms of carbonates from stone wastes in ternary blends with calcined clay, Constr. Build. Mater. 164 (2018) 265–274, https://doi.org/10.1016/j.conbuildmat.2017.12.240.
[44] L.A. Pereira-de-Oliveira, J.P. Castro-Gomes, P.M.S. Santos, The potential pozzolanic activity of glass and red-clay ceramic waste as cement mortars components, Constr. Build. Mater. 31 (2012) 197–203, https://doi.org/10.1016/j.conbuildmat.2011.12.110.
[45] G. Matias, P. Faria, I. Torres, Lime mortars with ceramic wastes: Characterization of components and their influence on the mechanical behaviour, Constr. Build. Mater. 73 (2014) 523–534, https://doi.org/10.1016/j.conbuildmat.2014.09.108.
[46] J. Dang, J. Zhao, W. Hu, Z. Du, D. Gao, Properties of mortar with waste clay bricks as fine aggregate, Constr. Build. Mater. 166 (2018) 898–907, https://doi.org/10.1016/j.conbuildmat.2018.01.109.
[47] R.D. Toledo Filho, J.P. Gonçalves, B.B. Americano, E.M.R. Fairbairn, Potential for use of crushed waste calcined-clay brick as a supplementary cementitious material in Brazil, Cem. Concr. Res. 37 (9) (2007) 1357–1365, https://doi.org/10.1016/j.cemconres.2007.06.005.
[48] E. Asensio, C. Medina, M. Frías, M.I. Sánchez de Rojas, Fired clay-based construction and demolition waste as pozzolanic addition in cements. Design of new eco-efficient cements, J. Clean. Prod. 265 (2020). doi:10.1016/j.jclepro.2020.121610.
[49] J.M. Paris, J.G. Roessler, C.C. Ferraro, H.D. Deford, T.G. Townsend, A review of waste products utilized as supplements to Portland cement in concrete, J. Clean. Prod. 121 (2016) 1–18, https://doi.org/10.1016/j.jclepro.2016.02.013.
[50] E. Aprianti S, A huge number of artificial waste material can be supplementary cementitious material (SCM) for concrete production – a review part II, J. Clean. Prod. 142 (2017) 4178–4194. doi:10.1016/j.jclepro.2015.12.115.
[51] DIN EN 12620:2013, Aggregates for concrete; German version EN 12620:2013, European Committee for standardization, 2013.
[52] DIN EN 196-1:2016-11, Methods of Testing Cement - Part 1: Determination of Strength, European Committee for standardization, 2016.
[53] DIN EN 206:2017-01, Concrete - Specification, performance, production and conformity; German version EN 206:2013+A1:2016, European Committee for standardization, 2017.
[54] DIN EN 12390-2/A20:2015-12, Testing hardened concrete - Part 2: Making and curing specimens for strength tests; Amendment A20, European Committee for standardization, 2015.
[55] DIN EN 933-1:2012-03, Tests for geometrical properties of aggregates - Part 1: Determination of particle size distribution - Sieving method; German version EN 933-1:2012, European Committee for standardization, 2012.
[56] H.M. Rietveld, A profile refinement method for nuclear and magnetic structures, J. Appl. Crystallogr. 2 (1969) 65–71, https://doi.org/10.1107/S0021889869006558.
[57] L.H. Grierson, J.C. Knight, R. Maharaj, The role of calcium ions and lignosulphonate plasticiser in the hydration of cement, Cem. Concr. Res. 35 (4) (2005) 631–636, https://doi.org/10.1016/j.cemconres.2004.05.048.
[58] N.N. Salim, A.L. Feig, Isothermal titration calorimetry of RNA, Methods. 47 (3) (2009) 198–205, https://doi.org/10.1016/j.ymeth.2008.09.003.
[59] E.J. Prosen, P.W. Brown, G. Frohnsdorff, F. Davis, A multichambered microcalorimeter for the investigation of cement hydration, Cem. Concr. Res. 15 (4) (1985) 703–710, https://doi.org/10.1016/0008-8846(85)90072-9.
[60] J.M. Díez, J. Madrid, A. Macías, Characterization of cement-stabilized Cd wastes, Cem. Concr. Res. 27 (3) (1997) 337–343, https://doi.org/10.1016/S0008-8846(97)00017-3.
[61] A. Tironi, M.A. Trezza, A.N. Scian, E.F. Irassar, Assessment of pozzolanic activity of different calcined clays, Cem. Concr. Compos. 37 (2013) 319–327, https://doi.org/10.1016/j.cemconcomp.2013.01.002.
[62] Y. Liu, S. Lei, M. Lin, Y. Li, Z. Ye, Y. Fan, Assessment of pozzolanic activity of calcined coal-series kaolin, Appl. Clay Sci. 143 (2017) 159–167, https://doi.org/10.1016/j.clay.2017.03.038.
[63] A. Bakolas, E. Aggelakopoulou, A. Moropoulou, S. Anagnostopoulou, Evaluation of pozzolanic activity and physicomechanical characteristics in metakaolin-lime pastes, J. Therm. Anal. Calorim. 84 (1) (2006) 157–163, https://doi.org/10.1007/s10973-005-7262-y.
[64] D.P. Bentz, A. Durán-Herrera, D. Galvez-Moreno, Comparison of ASTM C311 strength activity index testing versus testing based on constant volumetric proportions, J. ASTM Int. 9 (2012), 104138, https://doi.org/10.1520/JAI104138.
[65] DIN EN 12350-2:2019-09, Testing fresh concrete - Part 2: Slump test; German version EN 12350-2:2019, European Committee for standardization, 2019.
[66] DIN EN 12390-3:2019-10, Testing hardened concrete - Part 3: Compressive strength of test specimens; German version EN 12390-3:2019, European Committee for standardization, 2019.
[67] DIN EN 12390-13:2014-06, Testing hardened concrete - Part 13: Determination of secant modulus of elasticity in compression; German version EN 12390-13:2013, European Committee for standardization, 2014.
[68] DIN EN 14630:2007-01, Products and systems for the protection and repair of concrete structures - Test methods - Determination of carbonation depth in hardened concrete by the phenolphthalein method; German version EN 14630:2006, European Committee for standardization, 2007.
[69] C. Jakob, D. Jansen, N. Ukrainczyk, E. Koenders, U. Pott, D. Stephan, J. Neubauer, Relating ettringite formation and rheological changes during the initial cement hydration: a comparative study applying XRD analysis, rheological measurements and modeling, Materials (Basel) 12 (2019) 2957, https://doi.org/10.3390/ma12182957.
[70] U. Pott, C. Jakob, D. Jansen, J. Neubauer, D. Stephan, Investigation of the incompatibilities of cement and superplasticizers and their influence on the rheological behavior, Materials (Basel) 13 (2020) 977, https://doi.org/10.3390/ma13040977.
[71] M. Paul, Quality control of autoclaved aerated concrete by means of X-ray diffraction, (2018) 111–116. doi:10.1002/cepa.894.
[72] B.B. Sabir, S. Wild, J. Bai, Metakaolin and calcined clays as pozzolans for concrete: a review, Cem. Concr. Compos. 23 (6) (2001) 441–454, https://doi.org/10.1016/S0958-9465(00)00092-5.
[73] S. Wild, J.M. Khatib, L.J. Roose, Chemical shrinkage and autogenous shrinkage of Portland cement-metakaolin pastes, Adv. Cem. Res. 10 (3) (1998) 109–119, https://doi.org/10.1680/adcr.1998.10.3.109.
[74] D. Küchlin, O. Hersel, Betontechnische Daten - Augabe 2017, Ausgabe 20, HeidelbergCement AG, 2017.
[75] ASTM C311-05, Standard Test Methods for Sampling and Testing Fly Ash or Natural Pozzolans for Use in Portland-Cement Concrete, 2004. doi:10.1520/C0311-05.
[76] ASTM C618-12a, Standard Specification for Coal Fly Ash and Raw or Calcined Natural Pozzolan for Use in Concrete, ASTM International, 2012.
[77] P. Termkhajornkit, T. Nawa, K. Kurumisawa, Effect of water curing conditions on the hydration degree and compressive strengths of fly ash – cement paste, Cem. Concr. Compos. 28 (9) (2006) 781–789, https://doi.org/10.1016/j.cemconcomp.2006.05.018.

[78] J. Bai, S. Wild, B.B. Sabir, J.M. Kinuthia, Workability of concrete incorporating pulverized fuel ash and metakaolin, Mag. Concr. Res. 51 (3) (1999) 207–216, https://doi.org/10.1680/macr.1999.51.3.207.
[79] R. Siddique, Effect of fine aggregate replacement with Class F fly ash on the mechanical properties of concrete, Cem. Concr. Res. 33 (4) (2003) 539–547, https://doi.org/10.1016/S0008-8846(02)01000-1.
[80] M.A. Megat Johari, J.J. Brooks, S. Kabir, P. Rivard, Influence of supplementary cementitious materials on engineering properties of high strength concrete, Constr. Build. Mater. 25 (5) (2011) 2639–2648, https://doi.org/10.1016/j.conbuildmat.2010.12.013.